

# Thermal Oxidation-Induced Long Chain Branching and Its Effect on Phase Separation Kinetics of a Polyethylene Blend

Yan-Hua Niu,<sup>1</sup> Zhi-Gang Wang,<sup>2</sup> Xiao-Li Duan,<sup>1,3</sup> Wei Shao,<sup>1,3</sup> Du-Jin Wang,<sup>1</sup> Jie Qiu<sup>1,3</sup>

<sup>1</sup>CAS Key Laboratory of Soft Matter Chemistry, Department of Polymer Science and Engineering, Hefei National Laboratory for Physical Sciences at the Microscale, University of Science and Technology of China, Hefei, Anhui Province 230026 People's Republic of China

<sup>2</sup>CAS Key Laboratory of Engineering Plastics, Joint Laboratory of Polymer Science and Materials, Beijing National Laboratory for Molecular Sciences, Institute of Chemistry, Chinese Academy of Sciences, Beijing, 100190 People's Republic of China

<sup>3</sup>Graduate School, Chinese Academy of Sciences, Beijing, 100049 People's Republic of China

Received 2 April 2009; accepted 15 April 2010

DOI 10.1002/app.32664

Published online 27 July 2010 in Wiley Online Library (wileyonlinelibrary.com).

**ABSTRACT:** Thermal oxidation-induced long chain branching (LCB) during the molding processes for polyolefin copolymer poly(ethylene-co-butene) (PEB) and its blend with another polyolefin copolymer poly(ethylene-co-hexene) (PEH/PEB 50/50 blend, denoted as H50) was investigated mainly by rheological measurements. LCB with different levels could be introduced on PEB backbones by changing the molding temperature and/or molding time, which could be sensitively characterized by changes of rheological parameters, that is, storage modulus  $G'$  and complex viscosity  $\eta^*$ . Thermal oxidation-induced LCB of PEB in H50 samples could largely influence the phase separation

kinetics. Rheological measurements and phase-contrast optical microscope observations coherently indicated that thermal oxidation-induced LCB of PEB more or less retarded the development of phase separation and once it reached a certain level, the reduced chain diffusion even arrested phase separation. The decrease of mass-averaged molecular mass in H50 with high LCB level was ascribed to the reduced hydrodynamic volume. © 2010 Wiley Periodicals, Inc. *J Appl Polym Sci* 119: 530–538, 2011

**Key words:** polyolefin blend; long chain branching; phase separation kinetics

## INTRODUCTION

Polyolefins as the most widely used thermoplastics have gained a rapid progress during the past decades with the development of new catalysts and modified methods. The properties of polyolefins such as impact strength, thermal performance, chemical resistance, aging characteristics, and rheological behaviors can be largely improved through cross-linking or introducing long chain branching (LCB).<sup>1,2</sup> For semicrystalline polyolefins, LCB affects not only on the bulk properties, but also on the crystallization behaviors including crystallization rate, crystallinity, lamellar thickness, and even unit cell parameters of the crystals under both static conditions<sup>3</sup> and flow

fields,<sup>4</sup> which shows obvious effects on the final properties of their industrial products.

LCB of polyolefins can be either directly incorporated during synthesis<sup>5,6</sup> or introduced by irradiation or peroxides in a postreactor treatment.<sup>7,8</sup> In the former cases, the well-defined architecture with combination of LCB and narrow molar mass distribution can be obtained, especially with the development of single-site metallocene catalysts; whereas in the latter cases, the molecular structure appears more complex and cannot be precisely controlled, which in many cases is considered to satisfy the industrial requirements. Besides the intentionally introduced LCB, it is reported that thermal oxidative reactions tend to occur for polyethylene during the specific processing conditions or at higher short chain branching (SCB) level,<sup>9,10</sup> which also may lead to the possibility of LCB. It is commonly regarded that thermal oxidation-induced chain scission, LCB and/or cross-linking can simultaneously occur.

In general, three techniques are employed to detect the existence of LCB including high-resolution <sup>13</sup>C nuclear magnetic resonance (NMR) spectroscopy, size exclusion chromatography coupled with multiple-angle laser light scattering (SEC-MALLS), and rheology.<sup>11–13</sup> For those with LCB introduced by

Correspondence to: Z.-G. Wang (zgwang2@ustc.edu.cn).

Contract grant sponsor: "Innovation Project" of Center for Molecular Science, Institute of chemistry, Chinese Academy of Sciences; contract grant number: CMSAQ6 Y200718.

Contract grant sponsor: The National Science Foundation of China; contract grant number: 50803073.

Contract grant sponsor: The startup fund, University of Science and Technology of China.

peroxides<sup>14</sup> or having vinyl groups,<sup>6</sup> FTIR is often used as a convenient method to qualify the functional groups relating to LCB. However, except rheology, the above mentioned techniques show inherent shortcomings to detect a small amount of LCB. For example, NMR cannot distinct LCB with more than six carbons in length and the signals belonging to LCB are usually masked by that of short chain branching. SEC-MALLS also encounters difficulties at the low level of LCB especially for high molecular mass species. However, many investigations confirm that rheology is more sensitive than other traditional methods on detecting the low level LCB if the entwined molecular mass distribution can be excluded.<sup>11–13,15,16</sup> On the basis of the relations between chain topologies and rheological parameters extracted mainly from the model long chain branched polymers, rheological measurements have been widely used to quantitatively characterize the LCB levels. It has been proven that a slight LCB of polyolefin can lead to higher zero shear viscosity, lower onset shear rate for shear thinning, increased activation energy for flow, deviation of the van Gurp-Palmen curve ( $\delta - |G^*|$ ) from the linear ones, and obvious strain-hardening behavior in elongational flow.<sup>13,15</sup>

In this work, we take the advantages of rheological measurements to detect the subtle viscoelastic changes of two metallocene polyolefin copolymers, poly(ethylene-co-hexene) (PEH), poly(ethylene-co-butene) (PEB) and their blend (PEH/PEB 50/50 blend) by changing the molding conditions. The minimal level of LCB can be detected in PEB component (with higher SCB level), because of the active tertiary carbon atoms on its backbones. Considering that the relaxation and diffusion of polymer chains can be pronouncedly retarded by LCB, such structure is expected to further affect the phase separation kinetics when blending. Phase separation itself has been extensively investigated, however, as we know, the influences of thermal oxidation-induced LCB on phase separation kinetics during actual processing have been usually neglected. The reason is that so subtle structure changes induced by small levels of LCB cannot be sensitively detected by the traditional methods. This study is based on our previous investigations on phase separation kinetics of PEH/PEB blends,<sup>17–20</sup> and the purpose here is to explore the effects of the subtle chain structure changes in PEB and its blend with PEH (PEH/PEB 50/50 blend) on the phase separation kinetics.

## EXPERIMENTAL

### Materials and sample preparation

The polyethylene copolymers used in this study, PEH and PEB, were kindly supplied by ExxonMobil Chemical Company, New Jersey, USA and were the

same ones we used in our previous studies.<sup>19,20</sup> They were synthesized by metallocene catalysts and had relatively narrow molecular mass distributions ( $M_w/M_n \sim 2$ ) and uniform comonomer distributions. The mass-average molecular mass,  $M_w$ , was 112 kg mol<sup>-1</sup> for PEH and 70 kg mol<sup>-1</sup> for PEB determined by high temperature gel permeation chromatography (GPC). The mass density was about 0.922 g cm<sup>-3</sup> for PEH and 0.875 g cm<sup>-3</sup> for PEB, and the chain branch density was about 9 CH<sub>3</sub> per 1000 backbone carbons for PEH and 77 CH<sub>3</sub> per 1000 backbone carbons for PEB. The dried solution-precipitated PEH and PEB samples exhibited melting point temperatures,  $T_m$ , of 119.8 and 48.6°C, respectively (determined by differential scanning calorimetry at a heating rate of 10°C min<sup>-1</sup>).

The PEH/PEB 50/50 blend samples (denoted as H50) were prepared through coprecipitating of their xylene solutions. The solution temperature was first set at 120°C and kept for 30 min to ascertain sufficient dissolution of both PEH and PEB components. The solution temperature was then set at 100°C for about 8 h during the continuous stirring. Finally, the hot xylene solutions were poured into chilled methanol (ca. 0°C) with continuous stirring. After filtering, the obtained floccules were dried in air for 24 h and further dried in a vacuum oven at 60°C for 72 h until the solvent was completely removed. During the whole mixing process, solution temperature fluctuations (about 3–5°C) could not be avoided, which possibly led to thermal oxidation of PEB chains because of the high SCB level of PEB component. Thereby, through coprecipitating method, we not only obtained normal H50 samples in most cases but also obtained a series of H50 samples with different thermal oxidation-induced LCB levels, which could be detected by rheology because of its superior sensitivity to the minimal LCB levels. With increasing levels of LCB as measured by rheology, we denoted such a series of H50 samples as H50-1, H50-2, H50-3, H50-4, and H50-5 for further studies.

The dried floccules of H50 samples, PEH and PEB were then compression-molded into disks of about 1 mm in thickness and 25 mm in diameter for the rheological measurements. The molding temperature for H50 and PEH was 160°C, and the molding time was about 8 min. For PEB the selected molding temperatures were 70, 100, and 160°C, at which the molding time was 8 and 13 min, respectively.

### Rheological measurements

The linear viscoelasticity of H50 samples, PEH and PEB was measured by oscillatory shear rheometry on a TA AR2000 stress-controlled rheometer with 25 mm parallel plates. Isothermal frequency sweeps

covering the range of 0.01–500  $\text{rad s}^{-1}$  with strains of 2–5% (falling in the linear viscoelastic regime and ensuring sufficient torques) were performed at different temperatures for PEH, PEB, and H50 premolded at the above mentioned conditions. Dynamic time sweeps for H50 samples (H50-1, H50-2, H50-3, H50-4, and H50-5) were carried out at 130°C with a fixed frequency of 0.03  $\text{rad s}^{-1}$  and a given strain of 5%. Before the time sweeps H50 samples were firstly annealed at 160°C for 10 min to eliminate thermal histories. All rheological measurements were conducted under nitrogen blanket.

### Gel fraction determination

To examine the possible cross-linking, all PEB and H50 samples used in this study were extracted by Soxhlet extraction method with boiling xylene as solvent. Each sample was wrapped in a filter paper and a stainless steel 100-mesh screen. The extraction time was about 48 h. After extraction, the filter paper package was washed by methanol and then further dried in a vacuum oven at 60°C for 72 h. The percentage of insoluble portion was regarded as the gel fraction. The experimental results showed that there was no insoluble gel fraction remained after the extraction for all samples. Therefore, we concluded that cross-linking did not occur and the changes of rheological parameters were contributed to thermal oxidation-induced LCB.

### FTIR measurements

FTIR measurements for PEB samples premolded at different temperatures (70 and 160°C) were performed by using a Perkin-Elmer 2000 FTIR spectrometer in the wavenumber range of 500–2000  $\text{cm}^{-1}$ . After the rheological frequency sweep measurements, the PEB samples were removed from the parallel plates and subsequently compressed into thin films, which were further analyzed by FTIR.

### Gel permeation chromatography (GPC) measurements

The apparent molecular mass and molecular mass distribution (MWD) of H50 samples were determined by gel permeation chromatography (GPC) analysis (Polymer Laboratories, PL-GPC220, UK). Measurements were performed at 150°C with *o*-dichlorobenzene as the solvent.

### Phase-contrast optical microscope observation

For phase-contrast optical microscope observation H50 samples were hot-pressed between two cover glasses at 160°C to form films of about 20  $\mu\text{m}$  and

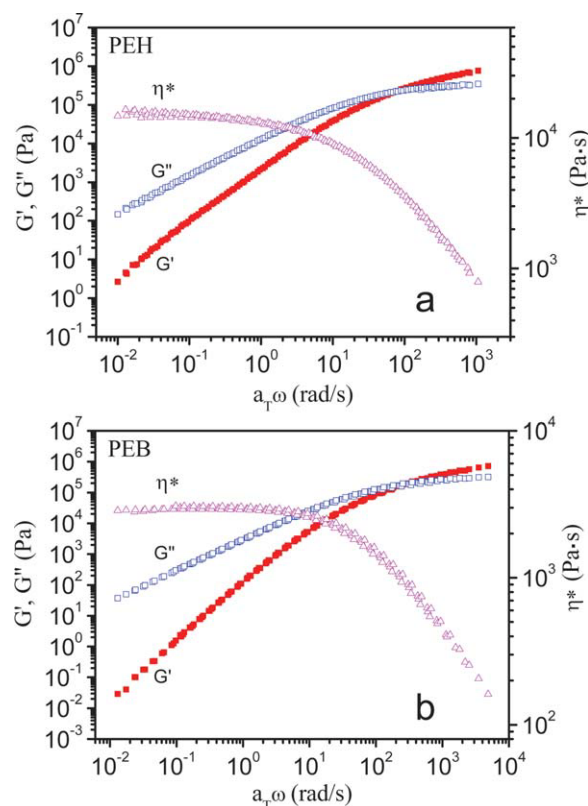


**Figure 1** Master curves for PEH (a) and PEB (b) at a reference temperature of 160°C. PEH and PEB samples were molded at 160 and 70°C for 8 min, respectively. [Color figure can be viewed in the online issue, which is available at [wileyonlinelibrary.com](http://www.interscience.wiley.com).]

then quenched to room temperature. The phase-contrast optical microscope observation of the films was carried out at 130°C after the films were annealed at 160°C for 10 min to eliminate thermal history by using an Olympus (BX51) optical microscopy coupled with a Pixera Penguin (150ES) CCD system. A Linkam (TMS 600) hot stage was used to control the sample temperatures.

## RESULTS AND DISCUSSION

Figure 1(a,b) show the master curves of modulus and complex viscosity for PEH and PEB at a reference temperature of 160°C, respectively. To avoid cross-linking, PEH and PEB samples were molded at 160°C and 70°C for 8 min, respectively. Excellent superposition of the moduli  $G'$  and  $G''$  for both two polymers is observed, which is consistent with that for other linear polyethylene.<sup>13</sup> Comparing the variations of complex viscosity  $\eta^*$ , it is seen that the curvature of  $\eta^*$  for PEH is slightly smaller than that for PEB, which indicates that the molecular mass distribution in the former is somewhat broader than the latter. In addition, the narrower Newtonian plateau for PEH also indicates its broader molecular mass



distribution. Because the applied temperatures during frequency sweeps exceed the glass transition temperature of polyethylene by far more than 100 K, the temperature dependence of the frequency shift factor  $a_T$  is expected to follow an Arrhenius equation:

$$\ln(a_T) = (-E_a/R)(1/T_0 - 1/T)$$

where  $E_a$  is the flow activation energy,  $R$  is the universal gas constant,  $T$  is the experimental temperature, and  $T_0$  is the reference temperature. The  $E_a$  values of PEH (36.6 kJ mol<sup>-1</sup>) and PEB (41.4 kJ mol<sup>-1</sup>) can be obtained through fitting, which as the characteristics of polymer chain mobility are independent of molecular mass but depend on the molecular architectures.<sup>13</sup> The above obtained  $E_a$  values of PEH and PEB show good agreement with that of metallocene linear low density polyethylenes (mLLDPE) reported by Hatzikiriakos.<sup>21</sup> His result indicates that a small amount of LCB of polyethylene can lead to the increasing of  $E_a$ , which can be divided into horizontal shift  $E_H$  and vertical shift  $E_V$ . For polyethylenes with no LCB, the vertical shift factor  $b_T$  is not necessary for obtaining a master curve, therefore,  $E_V$  is zero. In our investigation,  $b_T$  is approximately equal to 1, thus, LCB should not exist in our original PEH and PEB samples according to Hatzikiriakos.<sup>21</sup> However, Vega et al.<sup>15</sup> reported that the SCB density affects the flow activation energy and a high SCB level corresponds to a high  $E_a$  value. Therefore, it can be inferred that the high  $E_a$  value of PEB should be related to its high SCB level (77 branches/1000 C atoms).

### Thermal oxidation of PEB at different molding conditions

PEB is more sensitive to thermal oxidation than PEH during the molding process because of its obviously lower melting temperature and higher SCB level (with more active tertiary carbon atoms). In a recent report,<sup>22</sup> it is demonstrated that scission of PEB chains and formation of LCB can be tailored through changing processing conditions. Figure 2 compares the frequency sweep curves for PEH and PEB at 160°C (both samples were compression-molded at 160°C). At low frequencies,  $G'$  of PEH is close to, but not exactly reaching the terminal slope of 2, because of the molecular mass distribution,<sup>23</sup> whereas  $G'$  of PEB obviously deviates from the terminal behavior. It should be mentioned that this deviation has nothing to do with phase transition, because TTS works well as shown in Figure 1(b) when PEB is molded at much lower temperatures. Therefore we consider that such deviation is related to thermal oxidation of PEB, which induces a small amount of LCB on the PEB backbones during the

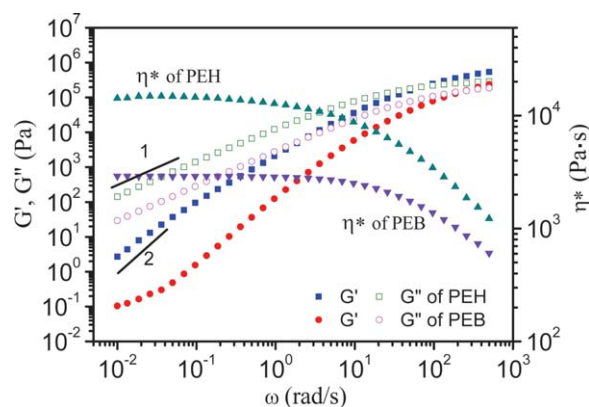


**Figure 2** Comparison of frequency sweep curves at 160°C for PEH and PEB samples premolded at 160°C for 8 min. [Color figure can be viewed in the online issue, which is available at [wileyonlinelibrary.com](http://wileyonlinelibrary.com).]

molding process. Compared with  $G'$ , both  $G''$ , and  $\eta^*$  are not so sensitive to such structure changes of PEB.

To confirm the above results, the effects of molding conditions (molding temperature and time) on the viscoelastic properties of PEB were examined. Figure 3(a) shows the frequency sweep curves at 160°C for PEB samples molded at different temperatures. It is clearly seen that at low frequencies (0.01–0.1 rad s<sup>-1</sup>)  $G'$  of PEB is largely affected by different molding temperature (with molding time of 8 min). For the sample molded at 70°C,  $G'$  can basically reach the terminal region at low frequencies. However, once the molding temperature increases to 100 or 160°C, the low frequency  $G'$  becomes higher and consequently deviates from the terminal slope. This deviation is a signature of thermal oxidation-induced LCB, which forms additional entanglements and essentially changes the long time relaxation process.<sup>12–15</sup> Figure 3(b) shows the effect of molding time (with molding temperature of 160°C) on the viscoelastic properties of PEB. As expected  $G'$  at low frequencies also increases with increasing molding time. Therefore, we consider that both the molding temperature and molding time can affect the thermal oxidation process of PEB and eventually affect the low frequency rheological parameters. With increasing molding temperature and molding time, thermal oxidation-induced LCB increases, and  $G'$  at low frequencies increases accordingly. Compared with  $G'$ ,  $G''$  is less affected by the molding conditions. It was reported that the van Gurp-Palmen plot ( $\delta - |G^*|$  curve)<sup>13,24–26</sup> is sensitive to the topology or architecture variations of polyolefins. However, the  $\delta - |G^*|$  curves for PEB samples molded at different temperatures [Fig. 3(c)] indicate no discernable contrast among the three samples. In other words, all data for PEB samples molded at different temperatures fall on one master curve for linear polyethylene, on

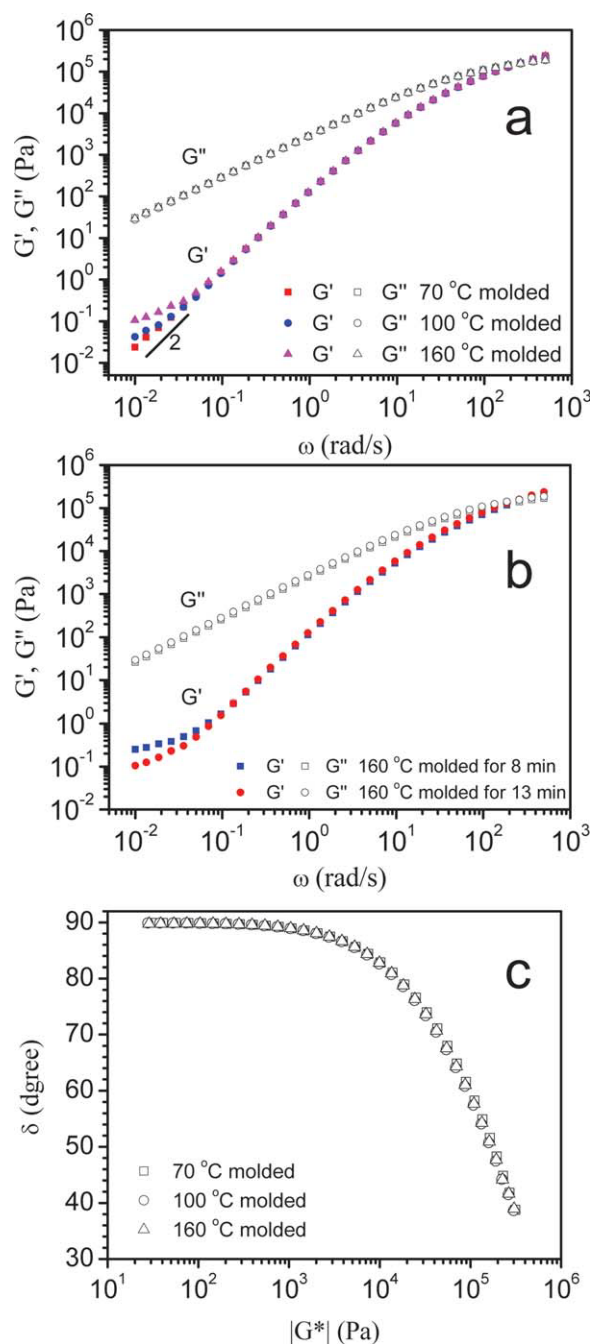


**Figure 3** Effects of molding conditions on modulus changes ( $G'$  and  $G''$ ) during frequency sweeps for PEB samples: (a) molding temperatures of 70, 100, and 160°C for 8 min; (b) molding time of 8 and 13 min at 160°C, and (c) the van Gurp-Palmen plots for PEB samples premolded at different temperatures. [Color figure can be viewed in the online issue, which is available at [wileyonlinelibrary.com](http://www.interscience.wiley.com).]

which  $\delta$  is nearly 90° for the low values of  $|G^*|$ . It is considered that the van Gurp-Palmen plot is not as sensitive as  $G'$  when LCB is subtle because  $|G^*|$  at low values is still dominated by  $G''$ .

We note here that, due to the relatively moderate molding temperature or time, no gel fractions were

obtained by gel extraction method for both PEB and H50 samples. During the molding process of polyethylene, if thermal oxidation occurs significantly, the expected carbonyl C=O group can lead to a characteristic absorption band ( $1721\text{ cm}^{-1}$ ) in the FTIR spectrum. In order to clarify this, FTIR analysis was performed on PEB samples molded at 70 and 160°C. Figure 4 shows the FTIR spectra of the two PEB samples. It can be seen that there are no distinct differences between the two spectra. For the spectrum of PEB sample molded at 160°C the characteristic absorption band of C=O group at  $1721\text{ cm}^{-1}$  cannot be found. As evaluated by Vega et al.,<sup>15</sup> even though FTIR has no particular difficulties on determining SCB, it is somewhat ambiguous to detect the slight LCB. In summary, all our above results demonstrate that the rheological measurement is much more sensitive on detecting the minimal low level of LCB than FTIR and gel extraction methods.

#### Effects of LCB on phase separation for H50

As PEB is the unstable component in PEH/PEB blends during processing, the thermal oxidation-induced LCB of PEB can largely affect the phase separation kinetics. In addition, thermal oxidative reaction in PEH/PEB blends is not easily controlled because not only the molding conditions but also the coprecipitating with temperature fluctuations or long mixing time can change the LCB levels. In terms of this complex situation, it is required to examine whether the chain structures have been changed after the sample undergoes coprecipitating or molding processes. Once the sample was prepared, we first performed a frequency sweep at 160°C to detect the possibility of LCB. As shown in Figure 5(a), H50 samples with different LCB levels present different viscoelastic properties. Among the

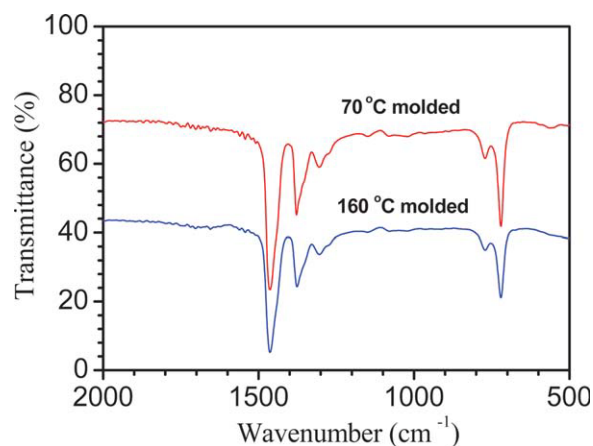


**Figure 4** FTIR spectra for PEB samples premolded at 70 and 160°C for 8 min, respectively. [Color figure can be viewed in the online issue, which is available at [wileyonlinelibrary.com](http://www.interscience.wiley.com).]

five samples, H50-1 is the normal sample with no detectable LCB and the slope of  $G'$  in the terminal region is about 2, which agrees with the scaling law for homogenous blends.<sup>23</sup> For H50-2 and H50-3,  $G'$  almost overlaps with that of H50-1 at frequencies higher than  $0.1 \text{ rad s}^{-1}$ , however, deviation of  $G'$  gradually occurs at frequencies lower than  $0.1 \text{ rad s}^{-1}$ , because of the appearance of small quantities of LCB. For H50-4, deviation of  $G'$  can be obviously observed at frequencies below  $0.1 \text{ rad s}^{-1}$ , whereas  $G''$  (not as sensitive as  $G'$ ) still superposes with that of H50-1, H50-2, and H50-3. Different from the above four samples, the thermal oxidation in H50-5 is more prominent as indicated by the fact that not only  $G'$  but also  $G''$  deviates from the normal values even at the intermediate frequency range. In addition,  $G'$  and  $G''$  are close to each other at low frequencies indicating that the sample in this case may be close to its critical gel point, which defines the instant of liquid-to-solid transition during chemical cross-linking of polymers.<sup>27</sup> For H50-5 the infinite insoluble network has not formed, which is evidenced by the gel extraction measurement, even if its elasticity is largely enhanced. Therefore, it is thought that the pronouncedly enhanced viscoelastic properties of H50-5 are only induced by a higher LCB level. Rheological measurements provide evidences to demonstrate that the relative LCB level gradually becomes higher and higher from H50-1 to H50-5 as indicated by the increasing  $G'$  or  $\eta^*$ .

Figure 5(b) illustrates the variations of complex viscosity  $\eta^*$  during frequency sweeps for the five H50 samples. It can be seen that the characteristic relaxation time from the Newtonian regime to non-Newtonian regime for H50-1 is about 10 s, and the zero viscosity,  $\eta_0$ , is 7250 Pa·s. For the samples with slight LCB levels, such as H50-2, H50-3, and even H50-4,  $\eta^*$  more or less deviates from the normal values of H50-1 at low frequencies. For the sample H50-5,  $\eta^*$  dramatically deviates from the Newtonian plateau even at the transition zone, and the curvature becomes negative at the low frequencies, because of the further thermal oxidation process during frequency sweep. Although it has been reported that the  $\eta^*$  curvature becomes negative within a broad range of frequency when the gelation is beyond the gel point,<sup>28</sup> which is valid for the balanced network, the negative curvature does not definitely indicate that the LCB-related network exceeds the critical gel point for the imbalanced or thermal oxidation ongoing process.

To provide more information about LCB levels of H50 samples, the van Gorp-Palmen plots<sup>24</sup> are displayed in Figure 5(c). For H50-1, H50-2, and H50-3, all the data fall on one curve close to that of PEB, except that the curvature is slightly smaller than PEB because of the broader molecular mass distribu-

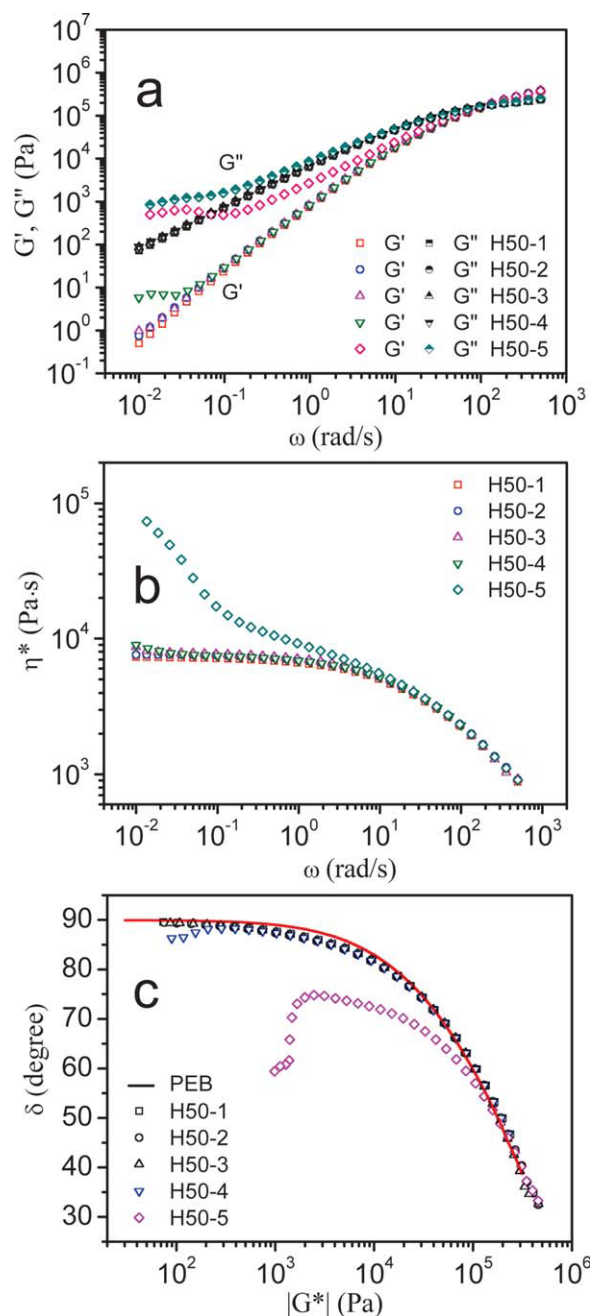


**Figure 5** Variations of (a)  $G'$  and  $G''$ , (b) complex viscosity  $\eta^*$ , and (c) the van Gorp-Palmen plots during frequency sweeps at 160°C for H50 samples denoted as H50-1, H50-2, H50-3, H50-4, and H50-5 with increasing LCB level. [Color figure can be viewed in the online issue, which is available at [wileyonlinelibrary.com](http://wileyonlinelibrary.com).]

tion upon blending with PEH.<sup>29</sup> This result indicates that despite PEH and PEB in H50 are well mixed, the LCB levels of PEB in H50 are too subtle to be reflected in the  $\delta$ - $|G^*|$  curves. However, the  $\delta$ - $|G^*|$  curves for H50-4 and H50-5, especially for the latter one, appear obviously different. More specifically,  $\delta$  of both two samples decreases at low  $|G^*|$  values, and the shape of  $\delta$ - $|G^*|$  curve for H50-5 is very similar to that of combed polyethylene,<sup>13</sup> which



indicates that H50-5 has the highest LCB level in the series of H50 samples. It should be kept in mind that even though H50-4 and H50-5 give obvious responses on the rheological parameters, the LCB levels are still too low to detect by the FTIR and gel extraction methods.

As known for polyethylene species, the chain scission and formation of LCB and/or cross-linking may occur simultaneously during processing.<sup>9,10</sup> With the appearance of LCB or cross-linking, the melt viscosity and molecular mass should increase, whereas the intrinsic viscosity should decrease if compared with the linear chains with the same molecular mass.<sup>22,30</sup> The increased melt viscosity is because of the LCB entanglements and the constrained relaxation. The decreased intrinsic viscosity is ascribed to the reduced hydrodynamic volume. Figure 6(a) compares the molecular masses of the five H50 samples. For the slight LCB samples or the linear one, the molecular mass basically keeps about the same, indicating that chain scission does not occur; whereas for H50-5 sample, the molecular mass obviously decreases, which seems to contradict with the increased zero shear viscosity. Nevertheless, the contradiction can be well interpreted as follows: the increased zero viscosity mainly contributes to the arm retraction of LCB, whereas the molecular mass determined by GPC is the apparent molecular mass, which can be largely influenced by the reduced hydrodynamic volume because the chains with the reduced hydrodynamic volume can be first excluded just like the low molecular mass species. Thus the apparent lower molecular mass of H50-5 also infers to its higher LCB level. Figure 6(b) displays the MWD curves for the H50 samples. It can be seen that the four H50 samples with low LCB levels show superposed MWD curves, while the H50-5 sample with high LCB level shows a shift of the MWD curve to the lower molecular mass side. This result is consistent with that shown in Figure 6(a).

To further investigate the effects of LCB on phase separation kinetics, the samples having undergone the frequency sweep at 160°C were subsequently quenched to 130°C and then isothermal time sweeps with a frequency of 0.03 rad s<sup>-1</sup> and a strain of 5% were carried out. In our previous investigations,<sup>19,20</sup> phase separation itself for PEH/PEB blends has been thoroughly explored through rheological experiments. Generally speaking, the physical origin of phase separation is because of concentration fluctuations, which involves various mechanisms, including spinodal decomposition (in unstable regime) and nucleation and growth (in metastable regime). Even the smallest concentration fluctuations in composition (lowering the free energy) can lead to spinodal decomposition, but larger concentration fluctuations are required to induce nucleation and

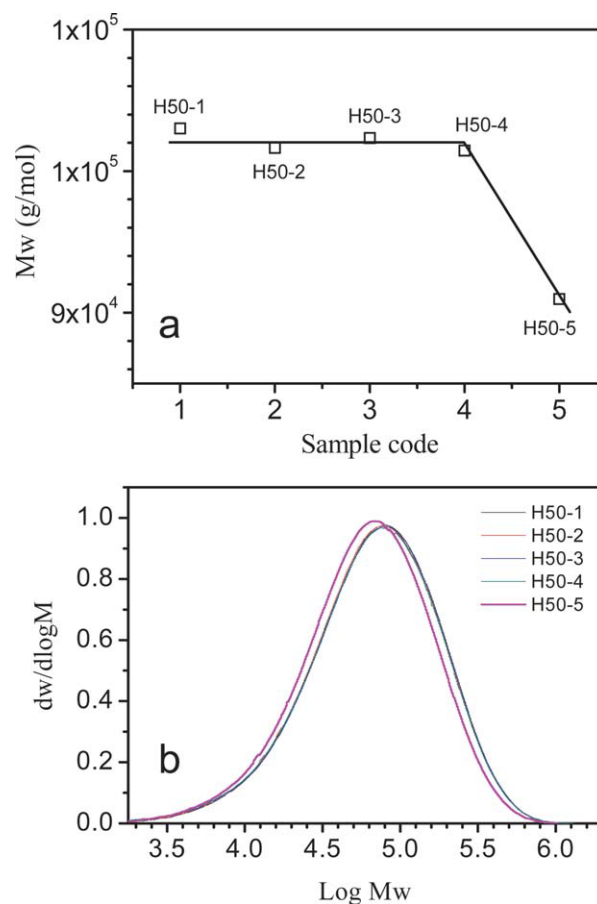


**Figure 6** Comparisons of (a) mass-averaged molecular mass and (b) MWD curves for H50 samples. [Color figure can be viewed in the online issue, which is available at [wileyonlinelibrary.com](http://wileyonlinelibrary.com).]

growth. For spinodal decomposition the cocontinuous phase domains are expected, while for nucleation and growth the droplet-matrix morphology can form. Due to the coupling effects of the reduced concentration fluctuations and decreased interfacial tension, the storage modulus should decrease obviously with spinodal decomposition progressing. However, if the polymer chain architecture changes the situation can be rather different, which will be discussed in more detail in the following section.

Spinodal decomposition is expected to occur at 130°C for H50 based on the previously determined phase diagram.<sup>19</sup> Figure 7 illustrates the time sweep modulus curves for the five H50 samples with different LCB levels. It can be seen that the values of  $G'$  for the five samples increase obviously with increasing LCB level, which is more evident for H50-4 and H50-5. For H50-1, H50-2, and even H50-3,  $G'$  all decreases with time, but the decreasing magnitude becomes smaller and smaller with increasing LCB level, whereas for H50-4 and H50-5,  $G'$  behaves to increase gradually with time. In general, for a normal blend sample with no LCB (say, H50-1),  $G'$

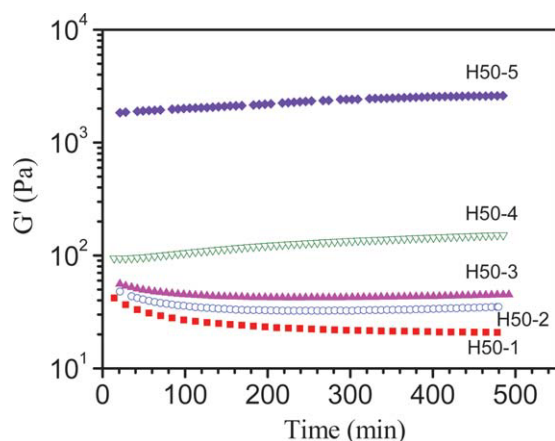


**Figure 7**  $G'$  evolution during time sweeps with a fixed frequency of  $0.03 \text{ rad s}^{-1}$  and a strain of 5% at  $130^\circ\text{C}$  for H50 samples denoted as H50-1, H50-2, H50-3, H50-4, and H50-5 with increasing LCB level. [Color figure can be viewed in the online issue, which is available at [wileyonlinelibrary.com](http://wileyonlinelibrary.com).]

decreases with phase separation time because of the reduced concentration fluctuations and decreased interfacial area.<sup>19,20</sup> However, formation of LCB due to thermal oxidation and phase separation are two correlated processes, in other words, formation of

LCB can dramatically affect phase separation. When the LCB levels are sufficiently subtle, such as H50-2 and H50-3, the LCB just increases the absolute values of  $G'$  and phase separation still plays a dominant role during the time sweep, so  $G'$  still decreases with phase separation time, but the phase separation process is somewhat delayed because of chain relaxation constrain. Whereas for the samples with higher LCB levels, for example, H50-4 and H50-5, because of simultaneous occurrences of chain scission and LCB as we have discussed above, the remnant long chain free radicals can lead to further formation of LCB at the phase separation temperature. Therefore, two scenarios can be predicted: one is that the thermal oxidation is not strong enough to stop phase separation, however, the effect of further formation of LCB on  $G'$  during the time sweep is stronger than that of phase separation, so the former one eventually overrules the latter one, hence  $G'$  increases with phase separation time; the other one is that the readily formed LCB entanglements hinder chain diffusion of PEB component, hence phase separation can hardly occur, and the further formation of LCB itself leads to  $G'$  increasing. Comparing the slopes of  $G'$  evolutions of H50-4 and H50-5, we can see that the slopes are almost equal to each other. Therefore, we

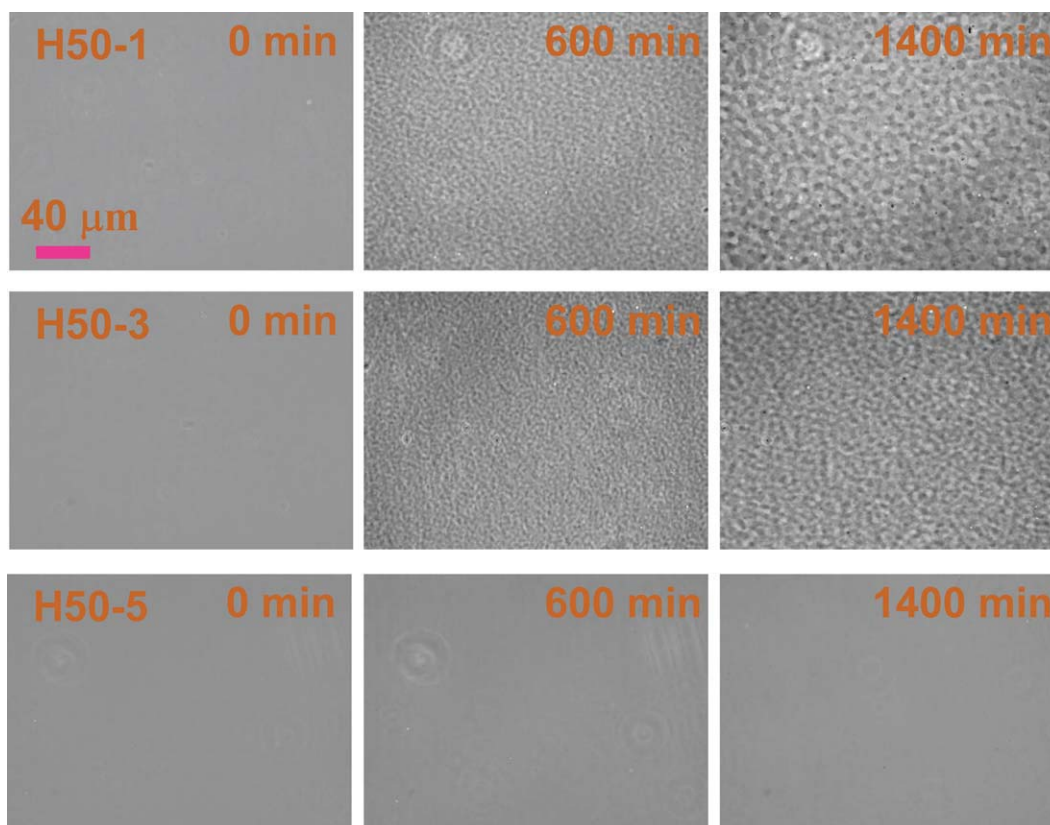


**Figure 8** Morphological evolution for H50-1, H50-3, and H50-5 during phase separation at  $130^\circ\text{C}$  observed by using phase-contrast optical microscope. [Color figure can be viewed in the online issue, which is available at [wileyonlinelibrary.com](http://wileyonlinelibrary.com).]



tend to argue that the increasing of  $G'$  for H50-4 and H50-5 is induced by the further formation of LCB, that is to say, the phase separation process has been completely hindered.

The morphological evolutions during phase separation give more direct supporting evidences to the above rheological results. Figure 8 shows the real-space phase separation evolution for H50-1, H50-3, and H50-5 samples at 130°C observed by using phase-contrast optical microscope. Similar to previous observations,<sup>17,18</sup> the characteristic cocontinuous morphology for the linear H50-1 sample can be clearly observed and the phase domains develop in a self-similar manner in the late stages of spinodal decomposition. With slight increase of LCB level for H50-3, the phase domains look somewhat smaller and progress more slowly than that of H50-1 at the same phase separation time, which indicates that slight LCB more or less retards the phase separation process by hampering chain diffusion. It is more interesting to find that for H50-5 with higher LCB level, there is no detectable phase separation signature even after 1400 min, indicating that the more condensed LCB entanglements can frustrate occurrence of phase separation. Therefore, the variations of  $G'$  for the H50 samples shown in Figure 7 are due to the obvious effects of thermal oxidation-induced LCB on phase separation. For H50-5, the prominent increasing of  $G'$  is from the contribution of further formation of LCB during time sweep process as phase separation is completely hampered. Comparing the results shown in Figures 7 and 8, one can conclude that rheological measurement is much sensitive to the earlier stages of phase separation than the optical method, which was previously discussed also.<sup>19</sup> In summary, the thermal oxidation-induced LCB of polyethylene has great effects not only on the viscoelastic behaviors but also on the phase separation kinetics of the blends, which is rather sophisticated and worth further investigations.

## CONCLUSIONS

The polyolefin copolymer PEB is unstable compared with PEH for molding process at temperatures above 100°C. Thermal oxidation-induced LCB on PEB and its blend (PEH/PEB 50/50 blend, denoted as H50) was detected by rheological measurements. Rheology is more sensitive to detect the minimal level of LCB than other methods such as FTIR, gel extraction method, and GPC. Gel extraction and GPC results indicate that there is no occurrence of cross-linking for all the PEB and H50 samples. For the H50 blends, the related rheological parameters of  $G'$  and  $\eta^*$ , and the  $\delta-|G^*|$  curves consistently behave obvious changes with increasing LCB level. The decrease of the molecular mass for H50-5 is due

to the LCB reduced hydrodynamic volume. The phase separation kinetics of H50 with different LCB level has been studied by rheological measurements and phase-contrast optical microscope observation. The results coherently indicate that the slight LCB more or less retards the development of phase separation. Once LCB is beyond a certain level, the readily formed condensed LCB entanglements prevent from chain diffusion of PEB, and then phase separation can hardly occur.

## References

1. Fujiyama, M.; Kondou, M.; Ayama, K.; Inata, H. *J Appl Polym Sci* 2002, 85, 762.
2. Su, F. H.; Huang, H. X. *Adv Polym Technol* 2009, 28, 16.
3. Tian, J. H.; Yu, W.; Zhou, C. X. *J Macromol Sci Phys* 2006, 45, 969.
4. Agarwal, P. K.; Somani, R. H.; Weng, W. Q.; Mehta, A.; Yang, L.; Ran, S. F.; Liu, L. Z.; Hsiao, B. S. *Macromolecules* 2003, 36, 5526.
5. Wang, W. J.; Yan, D. J.; Zhu, S. P.; Hamielec, A. E. *Macromolecules* 1998, 31, 8677.
6. Malmberg, A.; Liimatta, J.; Lehtinen, A.; Löfgren, B. *Macromolecules* 1999, 32, 6687.
7. Auhl, D.; Stange, J.; Münstedt, H.; Krause, B.; Voigt, D.; Lederer, A.; Lappan, U.; Lunckwitz, K. *Macromolecules* 2004, 37, 9465.
8. Liu, J. Y.; Yu, W.; Zhou, W.; Zhou, C. X. *Polymer* 2008, 49, 268.
9. Al-Malaika, S.; Peng, X. *Polym Degrad Stab* 2007, 92, 2136.
10. Al-Malaika, S.; Peng, X.; Watson, H. *Polym Degrad Stab* 2006, 91, 3131.
11. Stadler, F. J.; Piel, C.; Klimke, K.; Kaschta, J.; Parkinson, M.; Wilhelm, M.; Kaminsky, W.; Munstedt, H. *Macromolecules* 2006, 39, 1474.
12. Wood-Adams, P. M.; Dealy, J. M.; deGroot, A. W.; Redwine, O. D. *Macromolecules* 2000, 33, 7489.
13. Lohse, D. J.; Milner, S. T.; Fetters, L. J.; Xenidou, M.; Hadjichristidis, N.; Mendelson, R. A.; Garcia-Franco, C. A.; Lyon, M. K. *Macromolecules* 2002, 35, 3066.
14. Tian, J. H.; Yu, W.; Zhou, C. X. *Polymer* 2006, 47, 7962.
15. Vega, J. F.; Santamaría, A.; Muñoz-Escalona, A.; Lafuente, P. *Macromolecules* 1998, 31, 3639.
16. Shroff, R. N.; Mavridis, H. *Macromolecules* 1999, 32, 8454.
17. Wang, H.; Shimizu, K.; Kim, H.; Hobbie, E. K.; Wang, Z. G.; Han, C. C. *J Chem Phys* 2002, 116, 7311.
18. Zhang, X. H.; Wang, Z. G.; Dong, X.; Wang, D. J.; Han, C. C. *J Chem Phys* 2006, 125, 024907.
19. Niu, Y. H.; Wang, Z. G. *Macromolecules* 2006, 39, 4175.
20. Niu, Y. H.; Yang, L.; Shimizu, K.; Pathak, J. A.; Wang, H.; Wang, Z. G. *J Phys Chem B* 2009, 113, 8820.
21. Hatzikiriakos, S. G. *Polym Eng Sci* 2000, 40, 2279.
22. Liu, J. Y.; Yu, W.; Zhou, W.; Zhou, C. X. *Polymer* 2009, 50, 547.
23. Ferry, J. D. *Viscoelastic Properties of Polymer*; Wiley: New York, 1980.
24. Van Gurp, M.; Palmen, J. *Rheol Bull* 1998, 67, 5.
25. Stadler, F. J.; Kaschta, J.; Munstedt, H. *Macromolecules* 2008, 41, 1328.
26. Trinkle, S.; Walter, P.; Friedrich, C. *Rheol Acta* 2002, 41, 103.
27. Winter, H. H.; Mours, M. *Adv Polym Sci* 1997, 134, 165.
28. Winter, H. H. *Polym Eng Sci* 1987, 27, 1698.
29. Trinkle, S.; Friedrich, C. *Rheol Acta* 2001, 40, 322.
30. Jørgensen, J. K.; Stori, A.; Redford, K.; Ommundsen, E. *Polymer* 2005, 46, 12256.